Performance Analysis on Real-Time M-QAM Signal Transmission over a Fog-Induced FSO Link

Zun Htay[1], Carlos Guerra-Yanez[2], Zabih Ghassemlooy[3], Stanislav Zvanovec[2], Filipe M. Ferreira[1]

[1] Optical Networks Group, Department of Electronic and Electrical Engineering, University College London, London WC1E 7JE, UK
[2] Department of Electromagnetic Field, Faculty of Electrical Engineering, Czech Technical University in Prague, Prague 16627, Czech Republic
[3]Optical Communications Research Group, Faculty of Engineering and Environment, Northumbria University, Newcastle upon Tyne, NE1 8ST, UK

Abstract— This research conducts a performance analysis on a real-time experimental multi-quadrature amplitude modulation (M-QAM) free-space optical (FSO) system under different fog conditions. The study focuses on experimental investigations to assess the system's tolerance and performance. Experimental results will contribute to a comprehensive understanding of the reliability aspects of the M-QAM FSO system, offering practical insights that are vital for real-world applications in challenging atmospheric conditions

Keywords— Real-time, M-QAM, FSO, Fog

I. Introduction

Free-space optical (FSO) communication systems have emerged as a promising technology for high-data-rate, secure, and line-of-sight communication over the past few years. These systems utilize optical signals to transmit data through the atmosphere, offering advantages such as high bandwidth, low latency, and immunity to radio frequency (RF) induced interference [1]. By utilizing laser beams to transmit data through free space, FSO technology offers a compelling solution for applications demanding high bandwidth and secure communication, including military communications, urban connectivity, and last-mile solutions[2]. Despite its merits, the reliability of FSO systems is dependent on favorable atmospheric conditions. One of the primary challenges is the impact of fog, a meteorological phenomenon characterized by suspended water droplets near the Earth's surface [3],[4]. Fog introduces attenuation of optical signals, posing a significant obstacle to the seamless operation of FSO systems.

Previous studies have highlighted the need for a comprehensive understanding of how fog influences the performance of FSO systems, particularly concerning the choice of modulation schemes [5-7]. The modulation scheme plays a pivotal role in optimizing the trade-off between data rate and system robustness, making it imperative to evaluate the performance of specific modulation schemes under realistic atmospheric conditions.

In this paper, we evaluate the performance of an FSO system employing quadrature phase shift keying (QPSK) and different M-quadrature amplitude modulation (M-QAM) formats up to 1024-QAM under varying conditions. We implemented an adaptable transmitter (Tx) and receiver for automatic encoding and decoding of the M-QAMs signals using software defined radio environment by controlling the Tx (signal generator) and Rx (vector analyzer). In most research cases, FSO system performance analysis takes places with the evaluation of received power and error vector magnitude (EVM), signal to noise (SNR) or bit error rate (BER) in turbulent channels such as in [8], [9]. In this paper, we determined the system performance by the estimating EVM corresponding with the visibility (V) of the fog attenuation specifically. The rest of the paper is organized as follows: Section II describes the FSO system modeling and provides all the design considerations of the experimental demonstration and implementation of M-QAM FSO in fog induced environment. Section III explains the system performance analysis with the results and discussion on the measured data. Finally, Section IV concludes the paper.

II. System Modelling

The schematic block diagram of the experimental setup is presented in Figure. 1, and the key parameters are described in Table 1. The Tx unit consists of 1550nm laser and a Mach-Zehnder-modulator (MZM) driven by an RF signal generator. The signal Rx unit consists of a high-speed photodetector (PD) and with a transimpedance amplifier. Note that a green laser and a low-bandwidth receiver is used to determine the V of the link (i.e., fog attenuation experienced by the link). A 5-meter-long free space channel is obtained by collimating the single mode fibre (SMF) of the MZM, propagating over an indoor atmospheric chamber, and focusing it back to SMF before the PD. A fog machine is used to emulate the fog-induced channel. For the FSO alignment, an integrated kinematic collimator was used providing pitch and yaw adjustment, thus allowing the collimated beam to be easily steered while aligning the system. The detected RF signal is connected to a vector analyzer for evaluating the performance of the link. We have used a PC and an ethernet hub to adaptively change the modulation format of the signal generator and control the vector analyzer. The output of the auxiliar optical receiver is connected to a power meter, which is also connected to the PC via a USB cable. The considered key system parameters are given in Table 1.

In the context of optical communications, the received signal is given as:

$$y(t) = h(t) * x(t) + n(t), \quad (1)$$

where x is the transmitted signal, n is additive white Gaussian noise (AWGN) with variance σ_n^2, * is the convolution symbol and h is the channel gain, which is given by:

$$h = h_a h_t, \quad (2)$$

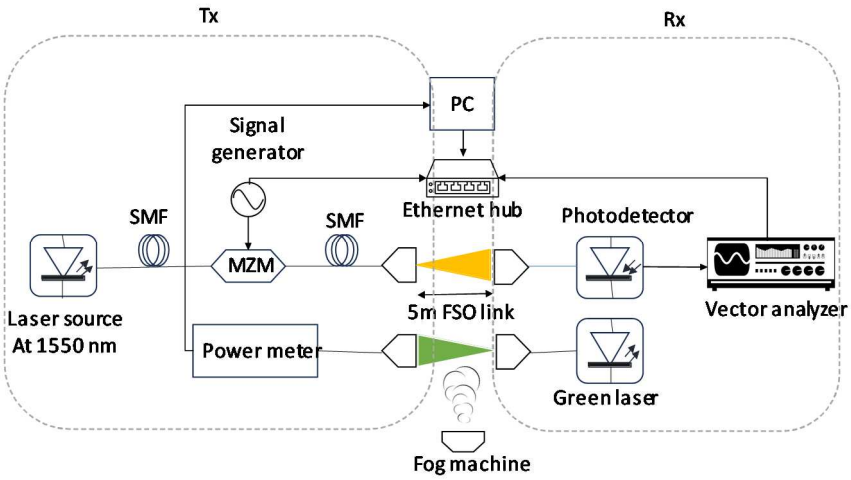

Figure 1: Schematic diagram.

where h_a and h_t are the attenuation constants due to the atmospheric channel and turbulence, respectively. For an FSO link, h_a is given by Beer's law as [10]:

$$h_a = e^{-\gamma l}, \qquad (3)$$

where l is the link length in m and γ is the attenuation coefficient in m^{-1}. The attenuation coefficient γ models the atmosphere and is the combination of absorption and scattering coefficients expressed as a function of wavelength. γ is given by [10]:

Table 1. Key system parameters.

Parameter	Value
Link length l	5 m
Data throughput (16, 32, 64, 128, 256 QAM)	400, 500, 600, 700, 800 Mbps
Transmitted output power P_{Tx}	~15 dBm
Rx collimator diameter D_{Rx}	24 mm
Tx collimator diameter D_{Tx}	24 mm
Tx beam divergence θ	0.016°
Optical wavelength λ	1550 nm
PD operating wavelength range	500 – 1630 nm
Photodetector (PD)	PIN
Responsivity of PD at 1550 nm	0.85 A/W
Noise equivalent power	24 pW/√Hz
PD bandwidth	~12 GHz
Collimator focal length f_l	37.13 mm

$$\gamma(\lambda) = \alpha_m(\lambda) + \alpha_a(\lambda) + \beta_m(\lambda) + \beta_a(\lambda), \qquad (4)$$

where, $\alpha_m(\lambda)$ and $\alpha_a(\lambda)$ are the molecular and aerosol absorption coefficients, respectively, and $\beta_m(\lambda)$ and $\beta_a(\lambda)$ are the molecular and aerosol scattering coefficients, respectively. The transmission wavelength in FSO is selected such that, it coincides with the atmospheric transmission window [11] hence, scattering governs the atmospheric attenuation coefficient and as a result $\gamma(\lambda) \approx \beta_a(\lambda)$. $\beta_m(\lambda)$, in which $\beta_a(\lambda)$ is expressed as [12]:

$$\beta_a(\lambda) = \frac{3.91}{V}\left(\frac{\lambda}{550\ \mathrm{nm}}\right)^{-q}, \qquad (5)$$

where, V is the meteorological visibility in km and q is the size distribution of scattering particles, for which the Kruse model is considered in this paper, as given by [13]:

$$q = \begin{cases} 1.6 & V > 50\ \mathrm{km} \\ 1.3 & 6\ \mathrm{km} < V < 50\ \mathrm{km} \\ 0.16V + 0.34 & 1\ \mathrm{km} < V < 6\ \mathrm{km} \\ V - 0.5 & 1\ \mathrm{km} < V < 1\ \mathrm{km} \\ 0 & V < 0.5\ \mathrm{km} \end{cases}, \qquad (6)$$

In our setup, we estimated the scattering coefficient of the channel using Beer's law:

$$\beta_a(\lambda) = \frac{\log\left(\frac{P_{Green-Rx}}{P_{Green-Max}}\right)}{l}, \qquad (5)$$

where $P_{Green-Rx}$ is the green laser power received for the channel condition under evaluation and $P_{Green-Max}$ is the maximum received power for a clear channel. From $\beta_a(\lambda)$ the atmospheric attenuation in dB/km is given by [14]:

$$L_{\mathrm{Atm}}\left(\frac{\mathrm{dB}}{\mathrm{km}}\right) = 4.343\beta_a(\lambda) \cdot l. \qquad (7)$$

III. Experimental Results and Discussion

We have developed an experimental testbed to investigate the reliability of the proposed M-QAM FSO link. The objective is to investigate the system

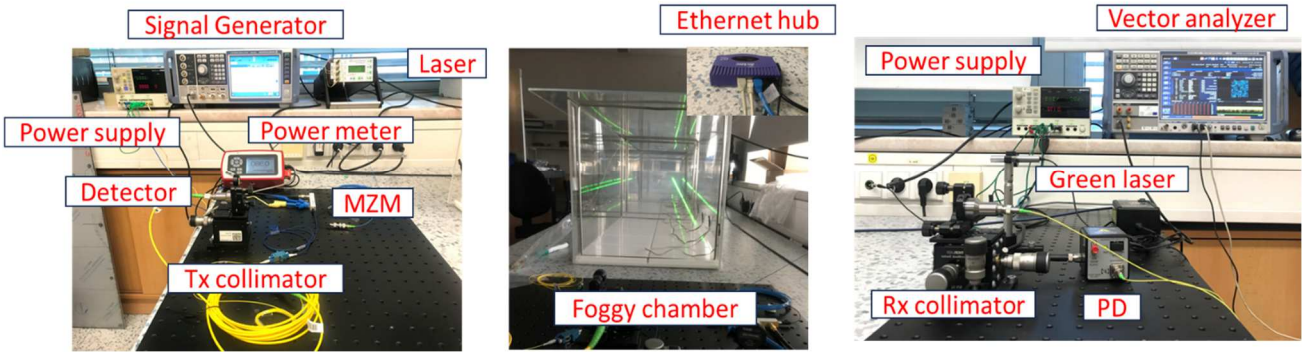

(a) (b) (c)

Figure 2: Experimental set up with (a) Tx. side, (b) channel setup and (c) Rx side.

performance by monitoring and controlling the system using a software platform without the need for changing the hardware platform and by only updating the software platform. The modulation formats are controlled and changed adaptively using a GNU Radio flow graph. We, therefore, investigate the performance of the proposed FSO link for different modulations under varying fog conditions. Figure. 2 is the experimental testbed based on Figure. 1. Figures. 2 (a), (b) and (c) are the Tx side, indoor atmospheric channel and Rx side respectively. A vector analyzer is used to compare the transmitted and received symbols. The system is tested for 30 seconds for three different fog conditions.

Table 2. The System Performance Metrics for the Clear, and Increasing Fog Density Conditions of V_1, V_2 and V_3.

Channel conditions	M-QAM	EVM (%)
Clear	16	2.8
	32	2.9
	64	2.9
	128	3
	256	3.1
V_1 $V \in (40,48)$ m	16	2.9
	32	3.1
	64	3.2
	128	3.27
	256	3.3
V_2 $V \in (23,40)$ m	16	3.61
	32	3.6
	64	3.7
	128	3.8
	256	4.02
V_3 $V<23$ m	16	4.5
	32	4.5
	64	4.8
	128	5
	256	5.2

Figures 3 (a) to (d) depict the constellation diagrams for five modulation formats (i.e., 16-, 32-, 64-, 128- and 256-QAM) for clear channel and three fog conditions with decreasing visibility ($V \in (40,48)$, $(23,40)$, and < 23 m), respectively. From Figure. 3 it can be seen that as the fog level increases there is a clear impact on the link performance.

We mainly performed the EVM measurements based on the constellation diagrams, which are for 16-QAM to 256-QAM. In general, the susceptibility to fog attenuation varies depending on the modulation scheme employed. Higher-order QAM, characterized by denser constellations and higher spectral efficiency, are particularly susceptible to fog-induced attenuation. The complexity of these schemes, with multiple amplitude and phase levels per symbol, increases their vulnerability to distortion and errors induced by fog. On the other hand, simpler modulation schemes like On-Off Keying (OOK) and Pulse Amplitude Modulation (PAM) also face challenges in foggy conditions but may exhibit lower susceptibility compared to higher-order QAM formats. While OOK relies on the presence or absence of light pulses and PAM varies the amplitude of optical pulses, both may experience attenuation and distortion due to fog, though to a lesser extent than higher-order QAM formats. Therefore, the choice of modulation scheme plays a crucial role in determining the performance and reliability of optical communication systems in foggy environments.

Table 2 presents the EVM results for the different QAM signals in different fog intensities, as a function of the V range. The dataset presented quantifies the influence of varying fog intensity and modulation states (M-QAM) on V in an FSO communication system. Here, and for the performance analysis, we take as reference the performance requirements standard to the early 5th generation technology for cellular networks, namely an EVM of 3.5% for 256 QAM [15] – whereas in the 3GPP specifications, the EVM limits of 17.5, 12.5 and 8% for

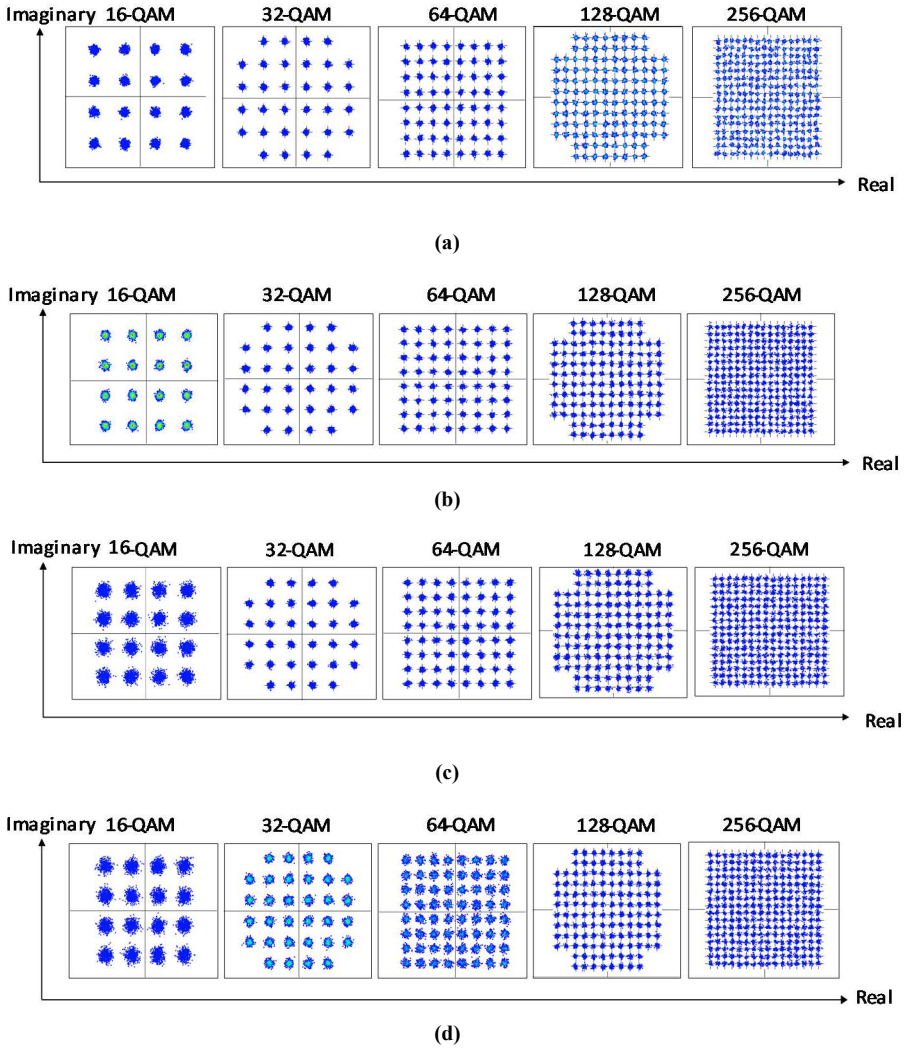

Figure 3: Constellation diagrams of 16, 32, 64, 128 and 256 QAM signals under (a) clear channel, (b) fog with $V \in$ (40,48) m, (c) fog with $V \in$ (23,40) m and, (d) fog with V<23 m channel.

4, 16, and 64 QAM, respectively, are presented by horizontal dashed lines [16]. For our testbed, Table2 shows that under optimal conditions characterized by a clear channel, the EVM values demonstrate that there is a notable degree of stability, indicating 2.9% for both 16-QAM and 32-QAM, with a slightly elevated yet consistent 3.1% for 256-QAM. Upon reaching $V \in$ (40,48) m, it can be seen from Table 2 that there is a noticeable change in the dynamics of the EVM. With results ranging from 3.1% for 64-QAM to 3.3% for both 32-QAM and 256-QAM, with noticeable measured rise in EVM values. Impact on receiver's ability to accurately decode symbols. The change in the environments condition characterized by $V \in$ (23,40) m introduces a more intricate narrative. The EVM values undergoes a gradual increase, reflecting the incremental impact of V. This upward trajectory reaches its peak at 4.02% for 256-QAM (see Table 2), indicating an elevated sensitivity of the system.

Yet, the most noticeable changes in the EVM are exhibited for V < 23 m, i.e., the highest fog induced attenuation. In this case, the EVM values experience a substantial escalation, ranging from 4.5% for 16-QAM and 32-QAM to 5.2% for 256-QAM – see Table 2. This amplification in EVM values points to an increased susceptibility of the system to V_3, potentially posing challenges to the integrity of the transmitted signals. In scenarios with moderate fog density (V_1 and V_2), where the degradation in signal quality is moderate, higher-order modulation schemes may still offer advantages in terms of spectral efficiency. However, in conditions of dense fog (V_3), simpler modulation schemes such as 16-QAM or 32-QAM may prove to be more robust, as they are less prone to distortion and inter-symbol interference. However, It's interesting to note that the resulted EVM values for 256-QAM and 512-QAM signals are well below 12.5%, which is a common threshold for 5G transmission standards [17].

We further analyzed the performance of 512 and 1024 QAM signals. However, we investigate that these advanced modulation complexities exhibit a notable lack of viability, even under conditions characterized by V_1. The EVM values for both 512-QAM and 1024-QAM surge considerably, reaching almost 8.5% and 20%, respectively. This observation underscores the inherent limitations associated with the application of 512-QAM and 1024-QAM, particularly in scenarios where atmospheric conditions introduce additional challenges. The increased symbol density and complexity of these modulation formats make them inherently more vulnerable to noise and distortion, resulting in higher EVM values. This observation underscores the trade-off between spectral efficiency and robustness in FSO communication systems operating in foggy environments. While higher-order modulation schemes offer increased data rates and spectral efficiency in clear weather conditions, their performance may deteriorate significantly in the presence of fog, necessitating careful consideration when selecting modulation formats for FSO links deployed in regions prone to atmospheric conditions.

IV. Conclusion

In conclusion, our analysis of the FSO communication system across diverse V conditions and modulation states facilitated by the flexibility of software defined radio as a tool has provided valuable insights. Importantly, our findings highlighted a correlation between higher modulation states and increased EVM, underscoring the need for a strategic balance in modulation complexities for effective FSO deployment across varied environmental scenarios. Further adaptable Tx and Rx schemes for different modulations and laser wavelengths using SDR in the reported setup is planned.

Acknowledgment

This work was supported by COST Action CA19111 (Newfocus) and the UKRI Future Leaders Fellowship [MR/T041218/1].

V. References

[1] Z. Ghassemlooy, W. Popoola, and S. Rajbandhari, *Optical wireless communications: system and channel modelling with Matlab®*. CRC press, 2019.

[2] D. Killinger, "Free Space Optics for Laser Communication Through the Air," *Opt. Photon. News,* vol. 13, no. 10, pp. 36-42, 2002/10/01 2002

[3] M. Uysal and H. Nouri, "Optical wireless communications — An emerging technology," in *2014 16th International Conference on Transparent Optical Networks (ICTON)*, 6-10 July 2014 2014, pp. 1-7

[4] A. K. Majumdar, Z. Ghassemlooy, and A. Arockia Bazil Raj, *Principles and Applications of Free Space Optical Communications*. Institution of Engineering and Technology, 2019.

[5] M. A. Ali, "Performance Analysis of Fog Effect on Free Space Optical Communication System," *IOSR Journal of Applied Physics,* vol. 7, pp. 16-24, 03/03 2015.

[6] J. Perez, Z. Ghassemlooy, S. Rajbhandari, M. Ijaz, and H. L. Minh, "Ethernet FSO Communications Link Performance Study Under a Controlled Fog Environment," *IEEE Communications Letters,* vol. 16, no. 3, pp. 408-410, 2012

[7] S. M. Yasir, N. Abas, S. Rauf, N. R. Chaudhry, and M. S. Saleem, "Investigation of optimum FSO communication link using different modulation techniques under fog conditions," *Heliyon,* vol. 8, no. 12, p. e12516, 2022/12/01/ 2022

[8] A. Maho *et al.*, *Experimental assessment of various optical communication chains for high-capacity optical feeder links* (International Conference on Space Optics — ICSO 2022). SPIE, 2023.

[9] D. N. Nguyen, J. Bohata, M. Komanec, S. Zvanovec, B. Ortega, and Z. Ghassemlooy, "Seamless 25 GHz Transmission of LTE 4/16/64-QAM Signals Over Hybrid SMF/FSO and Wireless Link," *Journal of Lightwave Technology,* vol. 37, no. 24, pp. 6040-6047, 2019

[10] E. Leitgeb, S. S. Muhammad, C. Chlestil, M. Gebhart, and U. Birnbacher, "Reliability of FSO links in next generation optical networks," in *Proceedings of 2005 7th International Conference Transparent Optical Networks, 2005.*, 7-7 July 2005 2005, vol. 1, pp. 394-401 Vol. 1

[11] W. O. Popoola, "Subcarrier intensity modulated free-space optical communication systems," Northumbria University, 2009.

[12] M. K. El-Nayal, M. M. Aly, H. A. Fayed, and R. A. AbdelRassoul, "Adaptive free space optic system based on visibility detector to overcome atmospheric attenuation," *Results in Physics,* vol. 14, p. 102392, 2019/09/01/ 2019

[13] L. D. M. P. W. Kruse, and R. B. McQuistan, *Elements of Infrared Technology: Generation, Transmission, and Detection* 1963.

[14] R. Paudel, Z. Ghassemlooy, H. Le-Minh, and S. Rajbhandari, "Modelling of free space optical link for ground-to-train communications using a Gaussian source," *IET Optoelectronics,* vol. 7, no. 1, pp. 1-8, 2013

[15] B. Witte. "Digital modulation basics, part 2: QAM and EVM.

[16] D.-N. Nguyen *et al.*, "M-QAM transmission over hybrid microwave photonic links at the K-band," *Opt. Express,* vol. 27, no. 23, pp. 33745-33756, 2019/11/11 2019

[17] J. Bohata, L. Vallejo, B. Ortega, and S. Zvánovec, "Optical CS-DSB Schemes for 5G mmW Fronthaul Seamless Transmission," *IEEE Photonics Journal,* vol. 14, no. 2, pp. 1-7, 2022